RSC Advances

PAPER

View Article Online
View Journal | View Issue

Cite this: *RSC Adv.*, 2014, **4**, 22266

Spacer-enhanced chymotrypsin-activated peptide-functionalized gold nanoparticle probes: a rapid assay for the diagnosis of pancreatitis†

Fang-Yuan Yeh,[a] I-Hua Tseng,[a] Shu-Hung Chuang[ab] and Chih-Sheng Lin*[a]

Received 10th January 2014
Accepted 6th May 2014

DOI: 10.1039/c4ra00258j

www.rsc.org/advances

Pancreatitis is the inflammation of the pancreas. Chymotrypsin, an indicator of pancreatic function, could serve as a biomarker for the diagnosis of pancreatitis. A gold nanoparticle (AuNP)-based fluorescence assay was fabricated in this study to assay the activity of chymotrypsin. Peptides labeled with fluorophores were conjugated onto AuNPs as a chymotrypsin-activated peptide-functionalized AuNP probe (AuNPs-peptide probe). The detection sensitivity of the AuNPs-peptide probe toward proteolytic activity was significantly increased by using spacer-enhanced peptides with specifically designed lengths and charges. The limit of detection of the designed AuNPs-peptide probe decreased, enabling detection at the pM level within a 15 min detection time. The AuNPs-peptide probe was used to evaluate chymotrypsin activity as an indicator of acute pancreatitis (AP) in a mouse model induced by cerulein challenge. The fecal chymotrypsin activity in cerulein-induced AP mice was significantly lower than that observed in controls. This is the first study to use an AuNPs-peptide probe for the diagnosis of pancreatitis using fecal specimens.

1. Introduction

Pancreatitis is a disease in which the pancreas experiences inflammation. It occurs when digestive enzymes are activated before they are secreted into the duodenum, allowing them to attack and damage the pancreas. In the United States, at least 250 000 patients are admitted to hospital each year for acute pancreatitis (AP), making it the second most common gastrointestinal disease. The incidence of pancreatitis continues to increase each year. The annual cost of caring for these patients is approximately $4–$6 billion.[1] Although the pathogenesis of AP is not fully understood, most hypotheses are based on the concept of the premature activation of digestive zymogens in the pancreas, leading to tissue necrosis by auto-digestion.[2] Measurements of plasma amylase and lipase levels are the most widely used methods for AP diagnosis.[3,4] However, false-positive amylase and lipase results could be caused by abnormal conditions,[5] and false-negative results could be obtained in hyperlipidemia[6] or diabetic ketoacidosis.[7,8] Furthermore, blood enzyme determinations are invasive tube tests that are not routinely available for use in the diagnosis of AP. Therefore, biochemical tests based on a single fecal sample serve can as a potential and valuable diagnostic alternative.[9] Although trypsin preactivation is the principal cause of pancreatitis, trypsin undergoes degradation in the distal small bowel, which make trypsin a bad fecal marker.[10] Previous studies have shown that chymotrypsin can serve as an indicator of pancreatic function and be related to pancreatic diseases.[11,12] Chymotrypsin is a serine protease secreted from the pancreas into the duodenum, where it becomes active. In the case of pancreas insufficiency secondary to pancreatitis, the secretion of the enzyme is markedly reduced; therefore, reduced chymotrypsin activity can be measured in pancreatitis. As with all fecal protease assays in conventional pancreatic function tests, fecal chymotrypsin can be utilized as a surrogate.[13]

In the past few decades, reports have described various proteases assays that are primarily based on liquid chromatography, substrate zymography, enzyme-linked immunosorbent assays (ELISA), radioisotopes, or chromogenic and fluorogenic substrates. However, these techniques are often associated with cost-ineffective features such as being time-consuming, expensive, discontinuous, or requiring specific instruments. Much attention has been paid to resonance energy transfer (RET) for *in vitro* and *in vivo* assays of proteases due to advances in fluorescence-based techniques.[14–16] Gold nanoparticles (AuNPs) are a potential nanomaterial for RET-based assays; AuNPs of less than 40 nm in diameter have the lowest scattering constant and therefore the highest potential to quench fluorescence.[17] AuNPs have a superior quenching efficiency in a broad range of wavelengths compared to other organic quenchers.[17,18]

We aimed to develop an efficient method to diagnose pancreatic disease by fecal samples. Therefore, AuNPs-peptide

[a]*Department of Biological Science and Technology, National Chiao Tung University, No.75 Po-Ai Street, Hsinchu 300, Taiwan. E-mail: lincs@mail.nctu.edu.tw; Tel: +886-3-5131338*

[b]*Department of Surgery, Mackay Memorial Hospital, Hsinchu Branch, Hsinchu, Taiwan*

† Electronic supplementary information (ESI) available. See DOI: 10.1039/c4ra00258j

probes for the detection of chymotrypsin activity were fabricated. The FITC-labeled peptides were conjugated onto AuNPs as chymotrypsin-activated peptide-functionalized AuNPs probe (*i.e.*, AuNPs-peptide probe), and a specially designed peptide spacer that could significantly increase the detection sensitivity was also introduced. The chymotrypsin activity in the feces of cerulein-induced AP mice was detected, and the results confirmed that the fabricated AuNPs-peptide probe could be effectively applied to the diagnosis of pancreatitis.

2. Results

2-1. Fabrication of chymotrypsin-activated peptide-functionalized AuNPs probes

The fabrication of the protease-activated AuNPs-peptide probes is illustrated in Fig. 1A. In each probe, specific FITC labeled peptides were self-assembled onto AuNPs through an Au–S bond by cysteine–gold interaction, of which Cys acted as an anchor. The fluorescence of FITC is quenched by AuNPs, and the fluorescence can only be recovered by protease activation, which hydrolyzes the peptide substrates allows FITC to diffuse beyond the efficient quenching distance from the nanoparticles. Fluorescence was measured using excitation/emission at 495/515 nm, and the change in fluorescence intensity was used to estimate protease activity.

2-2. Characteristics of the AuNPs-peptide probes

The sizes of the synthesized citrate-capped AuNPs were estimated by TEM to be 14.6 ± 2.4 nm (Fig. 1B) and by dynamic light scattering (DLS) to be 22 nm (Fig. 1C). The size of the AuNPs-P3 probe was estimated by TEM (Fig. 1D) and DLS (Fig. 1E) as 17.2 ± 1.1 nm and 29 nm in diameter, respectively. The citrate-capped AuNP and AuNPs-peptide probe demonstrated absorption spectra with a localized surface plasmon resonance (LSPR) band shift, with the absorption peak shifted from 520 to 525 nm (Fig. 1F). The chymotrypsin-activated AuNPs-peptide probe showed a similar absorption spectrum to that of the non-activated AuNPs-peptide probe.

Agarose gel electrophoresis was performed to identify the morphological changes in the AuNPs after fabrication and protease activation. Changes in the bands could be observed under visible light and UV-illumination. The gel shown in Fig. 2A (under visible light) indicates differences in migration between the citrate-capped AuNPs, the AuNPs-peptide probe, and the chymotrypsin-activated AuNPs-peptide probe. The UV-illuminated fluorescence band of the AuNPs-peptide probe without chymotrypsin activation was very weak; evidence for both free and bound peptide–FITC cleaved by chymotrypsin are also given in Fig. 2B (under UV-illumination).

2-3. Chymotrypsin activity assay by the AuNPs-peptide probes

AuNPs fabricated with different peptide substrates (listed in Table 1) were compared. Three fabricated AuNPs-peptide probes were used in the chymotrypsin activity assay with a 1 h detection time at 37 °C and pH 8.0. As shown in Fig. 2C, the recovered fluorescence intensity upon chymotrypsin activation was in the following decreasing order: AuNPs-P3 probe (6000 a.u.) > AuNPs-P2 probe (3000 a.u.) > AuNPs-P1 probe (500 a.u.). Notably, only 5 ng mL^{-1} chymotrypsin was applied to the AuNPs-P3 probe, whereas 500 ng mL^{-1} chymotrypsin was applied to the others. Further investigation of the optimal detection range and time are documented in Table 1. The required optimal detection time for each AuNPs-peptide probe decreased in the following order: AuNPs-P1 probe

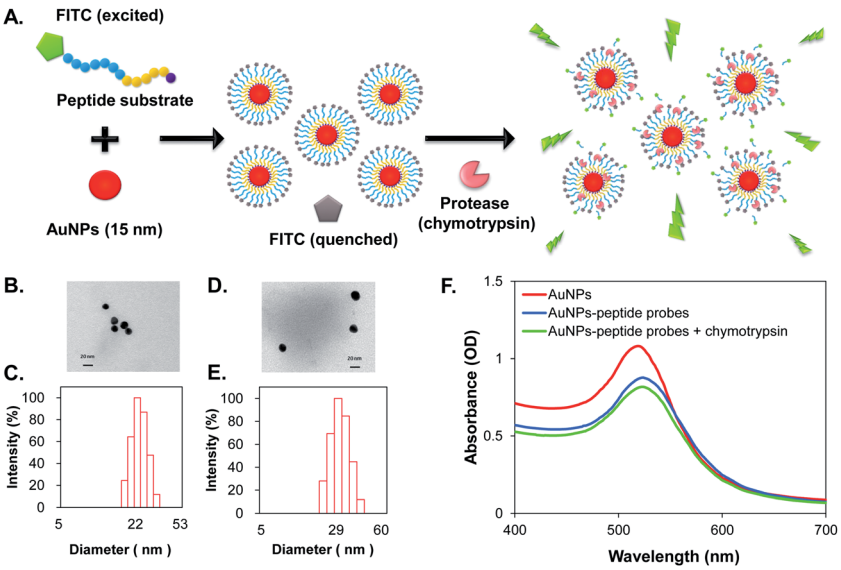

Fig. 1 (A) Schematic illustration of the protease activated fluorescent self-assembled AuNPs (AuNPs-peptide probe); (B) TEM image of citrate-capped AuNPs; (C) DLS result of citrate-capped AuNPs; (D) TEM image of AuNPs-P3 probe; (E) DLS measurement of AuNPs-P3 probe; and (F) absorption spectra of citrate-capped AuNP, AuNPs-P3 probe and chymotrypsin (500 ng mL^{-1} for 15 min at 37 °C) activated AuNPs-P3 probe.

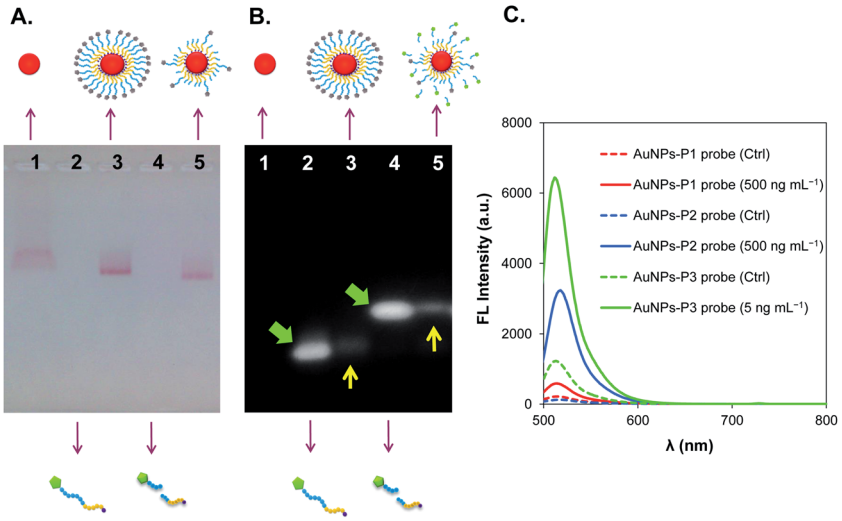

Fig. 2 (A) Agarose gel showing the migration of the bands of AuNPs and fabricated-AuNPs, which appear red in color; (B) the UV-illuminated gel shows the recovered fluorescence after chymotrypsin activation. For both (A) and (B), lane 1 = citrate-capped AuNPs; lane 2 = peptide substrate, P3; lane 3 = AuNPs-P3 probe; lane 4 = P3 digested by chymotrypsin; and lane 5 = AuNPs-P3 probe activated by chymotrypsin. (C) Fluorescence emission spectra of three different AuNPs-peptide probes activated by chymotrypsin after 1 h incubation.

Table 1 Peptide sequences corresponding to the chymotrypsin cleavage sites, the pH used during assembly onto the AuNPs, and the optimal detection range and time of the fabricated AuNPs-peptide probes for the assay of chymotrypsin activity[a]

No.	FITC-Acp-peptide	pI	AuNPs fabrication pH	Optimal detection range (ng mL^{-1})	Optimal detection time (min)
P1	GPL ↑ GL ↑ AG(Hyp)C	5.3	7.4	100–500	60
P2	GPL ↑ GL ↑ ARGGGGGC	7.8	10.0	25–300	30
P3	GPL ↑ GL ↑ ARDDDDDC	3.6	5.6	0.25–10	15

[a] The symbol (↑) indicates the potential cleavage sites cleaved by chymotrypsin. The pI of the peptide substrate was predicted using the online tools—Peptide Property Calculator, Genscript. The optimal detection range of the AuNPs-P1 probe showed a linear correlation of $\Delta FL = 0.78$ (chymotrypsin) + 7.29, $R^2 = 0.984$. The optimal detection range of the AuNPs-P2 probe showed a linear correlation of $\Delta FL = 4.95$ (chymotrypsin) + 82.35, $R^2 = 0.995$. The optimal detection range of the AuNPs-P3 probe showed a linear correlation of $\Delta FL = 506.69$ (chymotrypsin) + 90.82, $R^2 = 0.989$.

(60 min) > AuNPs-P2 probe (30 min) > AuNPs-P3 probe (15 min). Because the AuNPs-P3 probe showed superior sensitivity, the following experiments were conducted with this specific probe only.

To optimize the fluorescence assays using the AuNPs-peptide probe, the AuNPs-peptide probe concentration was a prime concern because the quenching effect of AuNPs is distance dependent. The concentration will affect the distance between particles, and that the adjacent particles can participate in quenching fluorescence of FITC. Different concentrations of the AuNPs-P3 probe (0.156–3.75 nM) were incubated with a fixed concentration of chymotrypsin (7.5 ng mL^{-1}) for 15 min at 37 °C. Fig. 3A shows that the optimal concentrations range of the AuNPs-peptide probe was 0.625–1.25 nM, whereas higher or lower concentrations resulted in poor performance, as indicated by the minor change in fluorescence intensity.

The specificity of the AuNPs-peptide probe was also investigated by comparing the use of serine proteases such as trypsin and chymotrypsin. Trypsin has a cleavage site at arginine (Arg) in P3. The AuNPs-P3 probe (1.25 nM) was incubated with various concentrations of trypsin and chymotrypsin (0.25–25 ng mL^{-1}), respectively, for 15 min at 37 °C and pH 8.0. Fig. 3B shows that the AuNPs-peptide probe was highly specific to chymotrypsin and displayed almost no change in fluorescence intensity in the presence of trypsin.

The time-dependent emission spectrum of the AuNPs-P3 probe upon treatment with 200 pM chymotrypsin is shown in Fig. 4A. The results indicated that the fluorescence intensity reached a steady state after approximately 80 min at 37 °C. The reaction kinetics of the AuNPs-P3 probe and chymotrypsin is an important parameter to in determining its biological applicability. To obtain the kinetic parameters, the fluorescence signal at 515 nm was plotted as a function of time (Fig. 4A, left). The pseudo-first-order rate, k_{obs}, was found to be 0.0424 s^{-1} by fitting the delta fluorescence intensity data with a single exponential function. The best fit with a single exponential function gave a $t_{1/2}$ of 16.3 min. Therefore, the detection time of the chymotrypsin assay using the AuNPs-P3 probe was determined to be 15 min. The concentration correlation was also displayed in Fig. 4B, where the AuNPs-P3 probe (1.25 nM) was incubated

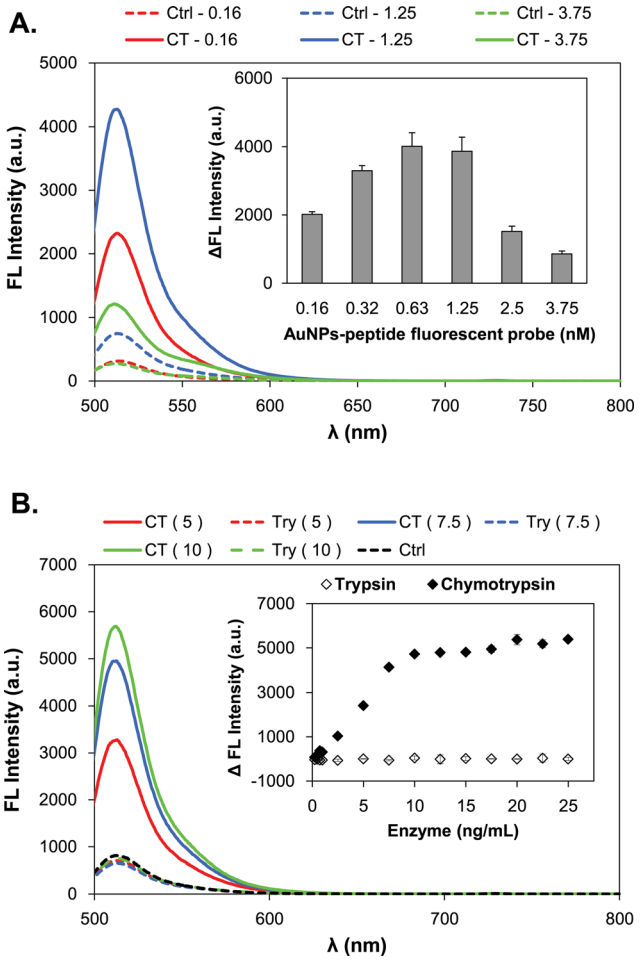

Fig. 3 Detection characteristics of the AuNPs-P3 probe. (A) Concentration optimization; and (B) detection specificity to serine proteases, including trypsin (open diamond) and chymotrypsin (close diamond). Error bars (SD) represent the data from three independent measurements.

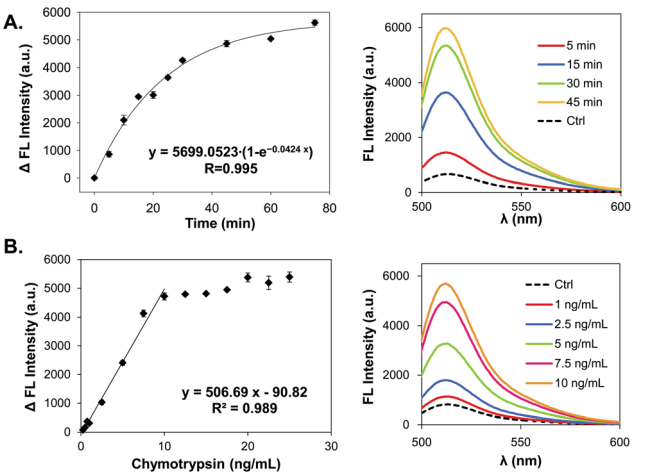

Fig. 4 Chymotrypsin activity assay using the AuNPs-P3 probe. (A) Time course of chymotrypsin (5 ng mL^{-1}, 200 pM) treatment. The solid line represents the best fit to a single exponential function, where $y = 5699.0523\ (1 - e^{-0.0424x})$ and $R^2 = 0.995$; and (B) the relationship between chymotrypsin concentration and fluorescence intensity in a 15 min detection time was determined. The linear correlation from 0.25 to 10 ng mL^{-1} of chymotrypsin was confident, for which $\Delta FL = 506.69$ (chymotrypsin) $- 90.82$ and $R^2 = 0.989$. Error bars (SD) represent the data from three independent measurements.

with various concentrations of chymotrypsin (0.1–25 ng mL^{-1}) for 15 min at 37 °C and pH 8.0. The results showed higher fluorescence intensities with increasing concentrations of chymotrypsin (Fig. 4B, right). The linear response to chymotrypsin, from 0.25 to 10 ng mL^{-1}, was well defined, with ΔFL intensity = 506.69 (chymotrypsin) − 90.82 and $R^2 = 0.989$ (Fig. 4B, left).

The stability of the AuNPs-peptide probes was evaluated and the results showed that the chymotrypsin assay using the AuNPs-P3 probe after 1 month of storage at ambient temperature was still above 90% compared to fresh use (data not shown).

2-4. Cerulein-induced AP mice

AP induction in the mouse model was conducted by a series of intraperitoneal cerulein injections. The mice were sacrificed at 8, 10, or 24 h after the first administration of saline (as control) or cerulein.

The collected plasma was analyzed by a Fujifilm clinical chemistry analyzer, in which of the amylase and lipase levels were determined. The plasma amylase levels of the cerulein-induced group were 27 and 49 (10^3 U L^{-1}) at the 8th and 10th h of sacrifice, respectively, which were significantly higher than of the values from the saline group (Fig. 5A). Moreover, the plasma lipase levels showed the same trend in the cerulein-induced group, with levels of 2.3 and 3.4 (10^3 U L^{-1}) at the 8th and 10th h of sacrifice, respectively, also significantly higher than of the values for the saline group (Fig. 5B). The saline group in each sacrificed period showed the similar amounts of plasma amylase (approximately 4000 U L^{-1}) and lipase (approximately 500 U L^{-1}) in each period. Both the plasma amylase and lipase levels showed at least a 3-fold increase compared to the controls, indicating that AP induction was successful in this study.

The pancreatic tissues of the mice were collected to confirm trypsin preactivation in AP occurrence. Extreme caution was exercised during the isolation of the pancreas because these tissues can be easily confused with fatty tissue (ESI Fig. S1A†), and beta cells can be identified by dithizone (DTZ) staining (ESI Fig. S1B and S1C†). The AuNPs-P3 probe was used to analyze pre-activated chymotrypsin in the pancreas. Fig. 5C shows that the pancreatic chymotrypsin level in the mice with cerulein-induced AP was approximately 2.8–3.6 ng chymotrypsin per mg total protein, which was significantly higher than that observed in the control group.

2-5. Diagnosis of AP by duodenal and fecal chymotrypsin

The collected eluent from the duodenum was analyzed using the AuNPs-P3 probe to determine the level of chymotrypsin. The amount of duodenal chymotrypsin in the mice with cerulein-induced AP showed a significant decrease in all three periods

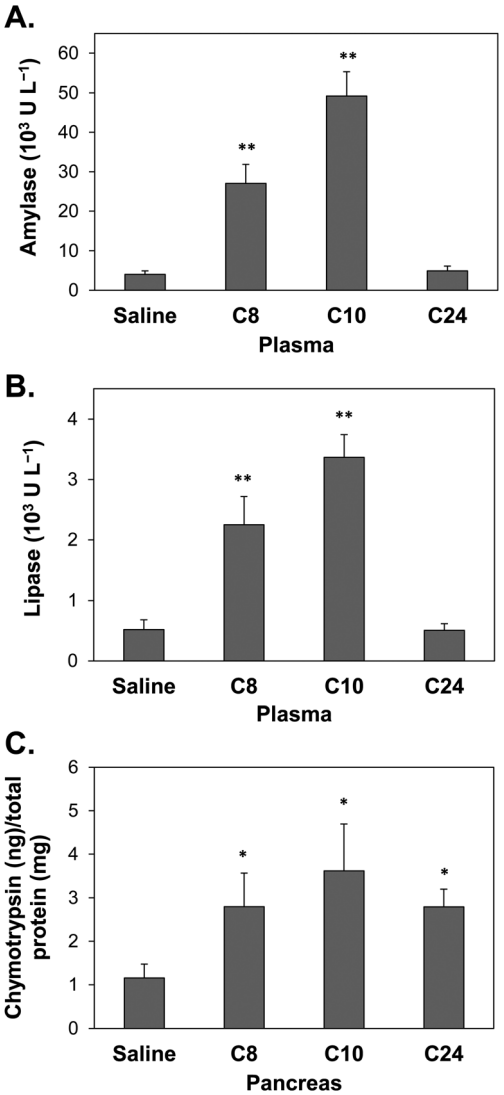

Fig. 5 Chymotrypsin activity in biological samples from mice sacrificed at 8 h (C8), 10 h (C10), or 24 h (C24) after the first administration of saline (control) or cerulein. (A) Plasma amylase, (B) plasma lipase, and (C) pancreatic chymotrypsin. Error bars (SD) represent data from three independent detections; * and ** indicate statistical significance at p-value <0.05 and <0.01, respectively.

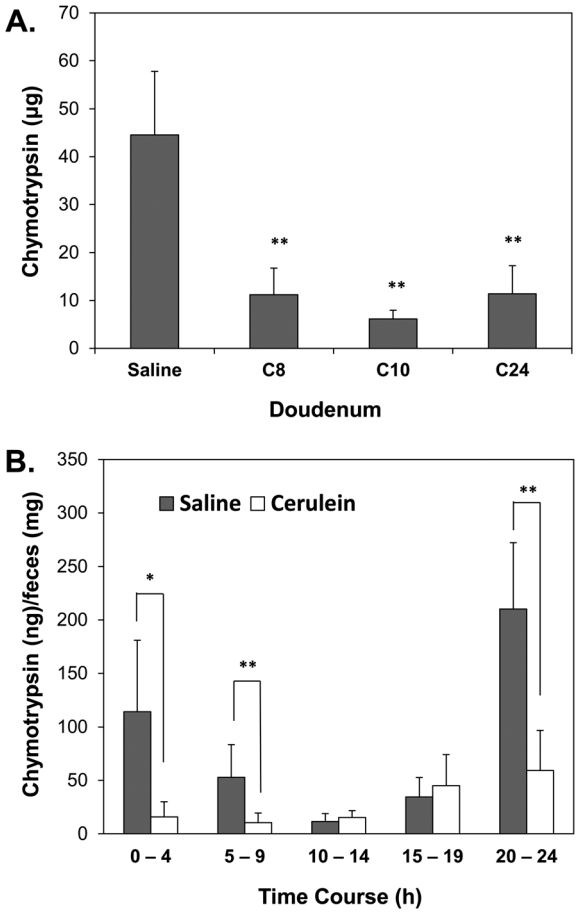

Fig. 6 (A) Duodenal chymotrypsin in mice with cerulein-induced AP; (B) 24 h time course of fecal chymotrypsin in a cerulein-induced AP mouse model. Every 5 h period was classified into one group; the grey bar indicates the saline group (control) and the white bar indicates the cerulein-induced group. Error bars (SD) represent the data from three independent detections; * and ** indicate statistical significance at p-value <0.05 and <0.01, respectively.

compared with that of the control group (Fig. 6A). The normal level of chymotrypsin was approximately 45 μg in the duodenal eluent, and significantly decreased to approximately 10 μg in the cerulein-induced group.

Fecal sample collection was conducted in 1 h-intervals for the entire 24 h time course. The supernatant collected from the fecal protein extraction was applied to the AuNPs-P3 probe (1.25 nM). Every 5 h period was classified into one group, thus generating the following groups: 0–4th h, 5–9th h, 10–14th h, 15–19th h and 20–24th h. The saline subjects showed changes in the cycle of chymotrypsin activity due to their diet. The 0–4th h, 5–9th h and 20–24th h groups from the mice with cerulein-induced AP showed a significantly lower chymotrypsin level compared with those of the control group (Fig. 6B).

3. Discussion

3-1. Fabrication of AuNPs-peptide probes

The use of protease-activatable fluorophore-conjugated AuNP probes has recently attracted considerable attention for the development of high-sensitivity detection methods for physiological activities. AuNPs 15 nm in size offer a high potential to quench fluorescence;[17] therefore, 15 nm AuNPs were used in this study, and fluorophores such as FITC, were conjugated to the terminus of the peptide substrates. The relationship between the AuNPs and the fluorophore is complex which at very close distances (<10 Å), radiative rate enhancement dominates; at intermediate distances (20–300 Å), energy transfer is the dominant process; and at very large distances (>500 Å), fluorescence oscillations due to dipole-mirror effects take precedence.[19] According to the size analysis results that the distance between AuNPs and FITC was approximately 13–35 Å, indicating quenching mechanism dominates this system. Based on the nanometal surface energy transfer model, the

quantum efficiency of the AuNPs-P3 probe was approximately 88.3–99.7%, theoretically.[20] The enzyme activity was determined by the recovered fluorescence, which was defined as the difference between the experiment group and the control group; hence the delta fluorescence intensity was able to eliminate the background effect.

The importance of peptide sequence design for the ligands coated on AuNPs has been previously studied,[21] because of the citrate-capped AuNPs showed poor stability (as shown in ESI Fig. S2B†). For a targetable probe used to detect protease activity, the peptide sequence must be limited to specific hydrolysis substrates. Therefore, it is essential to consider the overall effect of the peptide rather than only effect of the particular amino acid. It has been previously shown that increasing the length of the peptide can increase the stability of peptide-capped AuNPs.[22] Moreover, a previous study also proposed that peptide-modified AuNPs aggregation can be controlled by electrostatic repulsion between the peptides.[23] The aim of peptide design is to efficiently decrease the steric barrier caused by the densely packed layer of peptides on the AuNP surface to increase enzyme access to the cleavage site. Hence, this study examined two main concepts in peptide design, namely, length and charge. Three different peptide substrates were compared, with each possessing the same cleavage sites for chymotrypsin (Table 1). The length was tailored through the use of a spacer of repeating Gly units, $(Gly)_5$ (the difference between P1 and P2), and the charge was modified by substituting the non-charged $(Gly)_5$ spacer with a negatively-charged $(Asp)_5$ spacer (the difference between P2 and P3). The pH was adjusted according to the isoelectric point (pI) of the peptides to achieve a net negative charge on the peptide; hence to stabilize the AuNPs-peptide probe (data not shown). Besides, the pH of the AuNPs had no effect on aggregation (ESI Fig. S2A†).

AuNPs fabricated with peptide ligands can improve the stability of particles,[24] but the AuNPs-P2 probe stability showed was worse than that of the citrate-capped AuNPs (ESI Fig. S2C†). Nevertheless, the use of a stabilizer such as BSA, efficiently increased the stability of the AuNPs-P2 probe (data not shown). The negatively-charged spacer, $(Asp)_5$, promoted electrostatic repulsion between the particles and increased the stability of the AuNPs, which show good dispersion (ESI Fig. S2D†). DTT-based displacement was conducted to estimate the number of peptides conjugated to each AuNP. Our results showed that the number of peptide substrates (9–13 residues) conjugated to the 15 nm AuNPs was approximately 1000–1800 peptides per AuNP or 2.5–1.5 peptides nm^{-2}. Compared with previous reports involving a short peptide (2–6 residues) found approximately 200–900 peptides per AuNP 12–12.5 nm in size, our results showed a higher conjugation ratio.[22,25,26] In other words, the synthesized AuNPs-peptide probes were compactly packed with peptides. The advantages of the densely packed monolayers are as follows: (1) more loading peptides provide more chances for proteases to hydrolyze and activate the AuNPs-peptide probes, and (2) compact coverage increase the stability of AuNPs-peptide probes compared to that of citrate-capped AuNPs.

The zeta potential indicates the degree of repulsion between adjacent, similarly charged particles in dispersion. Colloids with a high zeta potential (negative or positive) are electrically stabilized, whereas those with low zeta potentials tend to coagulate or flocculate. A value of 25 mV (positive or negative) can be taken as the arbitrary value separating lowly-charged surfaces from highly-charged surfaces.[27] Park *et al.* showed that the zeta-potential value of AuNP to AuNPs-peptide–fluorescent protein changed from -26.44 ± 2.58 mV to 5.46 ± 2.44 mV.[28] Compared with our results, this value is less stable. The zeta potentials of the citrate-capped AuNPs and AuNPs-P3 probe in our study increased from -34.7 ± 13.8 mV to -39.2 ± 15.9 mV; this improvement can be attributed to the $(Asp)_5$ spacer.

3-2. Establishment of chymotrypsin activity assay using the AuNPs-peptide probe

A review of AuNPs-based biosensors for enzyme activity documented that the number of published AuNPs-based protease assays is relatively low (<100 publications) and only a few proteases (kinases, MMPs, and caspases) have appeared frequently to date.[29] This study presents a new target for AuNPs-based protease assays and a novel investigation of the effect of spacer length and charge on sensitivity. The specially designed peptide chain consisted of four elements: an anchor, a spacer, a sequence hydrolyzed by proteases, and a fluorophore. According to the results presented in Fig. 2C, the three fabricated probes showed different sensitivities in detecting chymotrypsin. The AuNPs-P2 probe showed a 5-fold increase in the delta fluorescence intensity compared to that observed in the AuNPs-P1 probe. It has been demonstrated that longer spacers on gold glyconanoparticles, which are AuNPs modified with a variety of saccharide molecules, enhance binding affinity to the target (lectins).[30] The results also corresponded to our observation that a longer spacer could result in a larger distance between the ligands at the same ligand density, hence reducing steric hindrance when the target approaches the ligands, making the ligands more accessible for interaction with the target.

The detection sensitivity of the AuNPs-P3 probe was superior (>100-fold) compared to that of the AuNPs-P2 probe. In our study, we proposed that the $(Asp)_5$ residues played a novel role as an extending anchor that decreased the steric hindrance to the enzyme and lowered the pI of the peptide, increasing particle stability. Asp also excluded the absorbed citrate on the AuNP, due to its repulsive interactions with the citrate carboxylates.[22] Hence, the repulsions between the chains and the citrate ions on the surfaces of the AuNPs maintained the dispersion of the peptides. The mechanism behind the increase in sensitivity using of a charged peptide spacer in functionalized AuNP-peptide probes remains to be explored. A few studies have shown that an enhancement of enzyme activity is possible using nanoparticles modified with polyvalent-conjugates. $(Arg)_6$ was used in the generation of cationic peptide formed nanoparticles that possessed significantly enhanced antimicrobial properties.[31] Functionalized dextranated magnetic nanoparticles with different valency of small molecules have shown an over 10^4-fold increase in avidity to the molecule-binding

protein.[32] Algar *et al.* have previously demonstrated that an increase in the charge of polyvalent QD–peptide conjugates can significantly enhance the sensitivity to trypsin cleavage of the peptide conjugates.[33] To the best of our knowledge, this study is the first report of the use of polyvalent peptide spacers to enhance enzyme activity in a AuNPs-based system for proteinase activity determination.

The enhancement of enzyme sensitivity through the use of spacers might also be due to the electrostatic complementarity between $(Asp)_5$ and chymotrypsin. A previous study showed that anionic functionalized nanoparticles were highly effective surface-based inhibitors of chymotrypsin; this activity was attributed to the electrostatic complementarity between the carboxylate end groups and the halo of cationic residues located around the periphery of the active site in chymotrypsin.[34]

Morphological changes in AuNPs with different treatments can be observed by agarose gel electrophoresis.[35] The mobility of the citrate-capped AuNPs increased upon modification with negatively-charged peptides, namely, the AuNPs-peptide probe. The mobility was further increased in the chymotrypsin activated AuNPs-peptide probe due to the loss of residues (Fig. 2A). The quenching phenomenon between AuNPs and FITC is confirmed in Fig. 2B; chymotrypsin activation is shown to turn on the fluorescence. The UV-illuminated gel shows that the fluorescent band with poorer mobility was attributed to the loss of the $(Asp)_5$ residues (lane 4 and land 5). The quenching effect of AuNPs is very important; therefore, the concentration of the AuNPs-peptide probe was considered due to its influence on the distance between individual particles. Fig. 3A shows the optimal concentration range; lower concentrations led to smaller changes in fluorescence intensity, and higher concentrations especially resulted in considerable decreases in intensity. The higher concentration likely had a negative impact due to the quenching effect whereas the lower concentration likely provided insufficient loading of the peptide substrates to detect protease activity. Additionally, the specificity of the AuNPs-peptide probe was investigated using the serine protease trypsin. Trypsin was chosen because it is structurally similar to chymotrypsin and follows the same secretion route in the digestive system. Trypsin has one cleavage site in the peptide substrate (P3); however, Fig. 3B shows that the AuNPs-peptide probe was unable to detect trypsin but exhibited high specificity to chymotrypsin.

3-3. Application of AuNPs-peptide probe to the diagnosis of AP

The AP mouse model was successfully established in this study (ESI S3†). Mice with cerulein-induced AP showed increased levels of plasma amylase and lipase. We aimed to confirm the presence of premature trypsin in AP based on increased pancreatic chymotrypsin activity.[36] Pancreatic acinar cells produce the inactive precursor of chymotrypsin, chymotrypsinogen, which is carried in the pancreatic juice through the pancreatic duct into the duodenum and then activated by trypsin. The chymotrypsin activity in the pancreas of cerulein-induced AP mice was analyzed by the AuNPs-P3 probe because of their high sensitivity. Fig. 5C supports the hypothesis that pancreatic chymotrypsin activity is significantly increased in mice with cerulein-induced AP, with chymotrypsin activity found to be increased by 3-fold compared to that of in the controls. Few works have discussed the elevated activity of chymotrypsin in the pancreas with AP. In a cerulein-induced rat model, a 3-fold increase in chymotrypsin activity has been observed relative to the normal,[36] which is consistent with our results. The reported maximal pancreatic injury at the 12^{th} h[37] was also similar to our findings that the 10^{th} h showed the highest level of pancreatic chymotrypsin.

However, there were inconsistencies in the pancreatic chymotrypsin, plasma amylase and lipase activity levels at the 24^{th} period, at which time levels of pancreatic chymotrypsin remained abnormal, whereas the other enzymes had reached normal levels. We were thus prompted to examine the two sources of chymotrypsin secretion. Chymotrypsin activity as an indicator to estimate the occurrence of pancreatitis usually refers to fecal chymotrypsin;[12] however, the chymotrypsin in duodenal fluid was also investigated in this study. The duodenal contents of cerulein-induced AP mice were collected after proper fasting to exclude the effect of food. The amount of chymotrypsin in mice with cerulein-induced AP significantly decreased in the duodenal fluid in all periods compared with that of the saline subjects (Fig. 6A). The duodenal chymotrypsin activity in mice with cerulein-induced AP showed a 25% decrease relative to that of controls. Acinar cell injury leads to pancreas malfunction, resulting in a decrease in chymotrypsin activity in the duodenum. This study is the first report to investigate the potential of duodenal chymotrypsin as a reliable index for AP in a mouse model. The duodenal chymotrypsin activity provides a direct estimate of pancreatic injury; however, it offers one disadvantage that it is invasive to obtain duodenal fluid. But for broader applications, the AuNPs-peptide probe has the potential in surgical applications, allowing real-time visualization of pancreatic juice leakage during surgery.[38]

Normally, for clinical diagnosis, 24 to 72 h stool collection is needed for protease determination.[12,39] The use of fecal chymotrypsin as an indicator of pancreatitis diagnosis usually refers to chronic pancreatitis; hence, we tried to find the applicability in acute pancreatitis. For stool productive species like mouse, that one collection of stool is not reasonable for experimental design; therefore, we conducted a 24 h collection of stool with 1 h intervals. Intra peritoneal cerulein injection can cause stomachache and loss of appetite; hence, fasting beforehand might encourage the mice to eat and therefore to produce stool. A continuous 24 h stool collection not only provided a time course for mouse digestion but also showed the change of fecal chymotrypsin activity in the mouse model of AP. Because of individual and digestion rate differences, the 24 h stool collection was categorized into groups to average performances. The saline subjects showed a cycle change in chymotrypsin activity due to their diet. Base on overall average, the cerulein-induced group had lower fecal chymotrypsin activity than that of controls, which the dividing fecal chymotrypsin as abnormal status was approximately 30 ng mg^{-1} of stool. Especially the $0–4^{th}$ h, $5–9^{th}$ h and $20–24^{th}$ h groups of

cerulein-induced AP mice showed significantly lower fecal chymotrypsin activity (30%) relative to that of controls (Fig. 6B). It has been proposed that a fecal chymotrypsin below 3 U g^{-1} of stool (approximately 75 ng mg^{-1} of stool) suggests advanced chronic pancreatitis in human.[40] The advantage of fecal chymotrypsin over duodenal chymotrypsin is its ease of specimen collection. Moreover, based on the high sensitivity of the AuNPs-P3 probe, only 10–20 mg of feces is required for the assay, making monitoring feasible.

4. Experimental section

4-1. Chemicals

All chemicals were analytical reagent grade and used without further purification. Sodium citrate ($C_6H_5Na_3O_7 \cdot 2H_2O$), calcium chloride ($CaCl_2$), Triton X-100, hydrogen tetrachloroaurate(III) ($HAuCl_4 \cdot 3H_2O$), Brij™ 35 solution 30% (w/v), polyethylene glycol (#P2139, Mw 8000), DL-dithiothreitol (#D5545), dithizone (#D5130), collagenase type I (#C9891), chymotrypsin (#C4129) were obtained from Sigma-Aldrich (St. Louis, MO, USA). HPLC-grade acetonitrile (ACN), were obtained from Merck (Darmstadt, Germany). Tris–HCl, Dulbecco's phosphate buffered saline (DPBS), were purchased from Invitrogen (San Diego, LA, USA). Sodium chloride was purchased from USB (Cleveland, OH, USA). Nanopure water (18 MΩ cm; Millipore, Bedford, MA, USA) was used in all experiments and to prepare all buffers.

4-2. Apparatus

Absorption spectra of AuNPs and fabricated-AuNPs were analyzed by UV-Vis spectrophotometer (SpectraMax 190; Molecular Devices Corporation, Sunnydale, CA, USA). Absorbance values of protein assay were recorded at 595 nm using a UV-Vis spectrophotometer (Molecular Devices Corporation). The fluorescence signals of AuNPs-peptide probe were analyzed by fluorescence spectrophotometer (F-2700; Hitachi, Tokyo, Japan). Enzyme activities in plasma/serum were analyzed by Fujifilm clinical chemistry analyzer (FUJI DRI-CHEM 3500; Fujifilm Corporation; Tokyo, Japan). The gel electrophoresis analyses were performed with horizontal electrophoresis system (Mini-Sub Cell GT; Biorad, Corston, UK). Microscope equipped with a high-resolution video camera (BX51; Olympus, Tokyo, Japan). Size examination of AuNPs and fabricated-AuNPs were examined by transmission electron microscopy, TEM (JEM-1230; JEOL, Tokyo, Japan) operated at 100 kV and equipped with CCD camera, and dynamic light scattering, DLS (Brookhaven Instruments Corporation, Holtsville, NY, USA). Particles analyzed by Zetasizer Nano (Malvern Instruments, Worchestershire, UK) and use disposable solvent resistant micro cuvette (ZEN0040) at room temperature.

4-3. Preparation of AuNPs

AuNPs were prepared by citrate reduction method according to the reported procedure.[35,41] Colloidal AuNPs (15 nm in diameter) were prepared as follows: 50 mL of 1 mM chloroauric acid solution was heated with oil bath till boiling, and followed by the addition of 5 mL of 38.8 mM sodium citrate solution. The color of the solution would turn from yellow to color less to black and to wine red. After the solution was cooled to room temperature, the product of 15 nm AuNPs solution was preserved at 4 °C. The size of AuNPs was confirmed by TEM and DLS, and the concentration was estimated by Beer's law with absorbent peak at 520 nm with an extinction coefficient of 3.94×10^8 M^{-1} cm^{-1}.

4-4. Preparation of AuNPs-peptide probes

Three peptide substrates were used in the protease activated AuNPs-peptide probes and the sequences were documented in Table 1. The difference between peptide#1 (P1, GPLGLAG(Hyp)C) and peptide#2 (P2, GPLGLARGGGGGC) is length which the anchor increase with a spacer of repeating glycine, $(Gly)_5$. The difference between P2 and peptide#3 (P3, GPLGLARDDDDDC) is the spacer of non-charged $(Gly)_5$ to negatively-charged aspartic acid, $(Asp)_5$. However, three of them have the same cleavage sites to chymotrypsin. The peptide–FITC was synthesized commercially by Genesis Biotech (Taipei, Taiwan). The peptide included a cysteine (Cys) in the C-terminal containing a thiol group (–SH) which could conjugate on to AuNPs through Au–S bond. The probes were synthesized as following: the prepared AuNPs were adjusted to proper pH by 1 N HCl or 1 N NaOH and then the concentration was adjusted with ddH_2O to OD = 1, which was 980 μL of 2.5 nM AuNPs. AuNPs were mixed with 10 μL of 1 mg mL^{-1} peptide–FITC and 10 μL of 0.01 M phosphate buffer containing 0.1% SDS and 0.3 M NaCl, and then the mixture were shaken for 12 h, 40 × *g* at room temperature. AuNPs-peptide probes were purified by two rounds of centrifugation. After first centrifugation (10 000 × *g* for 20 min), the supernatant was carefully removed and added 500 μL 2% (wt/wt) PEG. After the second centrifugation (11 000 × *g*, for 20 min), the supernatant was removed and resuspended with ddH_2O (AuNPs-P3 probe) or 0.1% BSA (AuNPs-P1 and AuNPs-P2 probes).

4-5. Gel electrophoresis of AuNPs-peptide probes

Gel electrophoresis analysis modified from Hanauer' protocol was used to confirm the change of AuNPs after fabrication and protease (chymotrypsin) activation.[40] The morphological change could be observed from visible red bands of AuNPs and UV-illuminated fluorescent bands. Agarose gels (1.5%) were used and prepared with 0.5× TBE buffer. All samples loaded with 35% glycerol for increasing density as the ratio of 7 : 1 (in volume). The citrate-capped AuNPs mixed with very small amount of 10% SDS (1 μL) for migration. The gels were run in a horizontal electrophoresis system for 30 min at 110 V in 0.5× TBE buffer. Gel images were taken by a digital camera under visible light and UV-light; besides, the images might be processed with small linear contrast adjustments in order to obtain the true representation.

4-6. Dithiothreitol-based displacement

Dithiothreitol (DTT)-based displacement was utilized for separating peptides from their AuNP. DTT will reactively displace

the ligands from surface sites because it is much more reactive toward AuNP compared with most ligands of interest.[42] In this study, the conjugate ratio of peptide–FITC to AuNPs could be quantified by fluorescence intensity. Fluorescence was measured using excitation/emission of 495/515 nm. DDT-based displacement was conducted as following: prepared 50 mg mL^{-1} DTT (dissolved in pH 6.5 PB buffer, 0.1 M) and then added 500 μL DTT to suspend AuNP probe sediment (0.625 nM) for 12 h incubation at room temperature. The total fluorescence of loading peptide substrates was defined after proper dilution and acquired a linear correlation between peptide–FITC concentration and fluorescence intensity, and the supernatant of DTT displacement also processed with same procedure to acquire the linear correlation. Dilution buffer was TTC buffer (50 mM Tris, 10 mM $CaCl_2$, 150 mM NaCl and 0.05% Brij 35, pH 8.0).

4-7. General procedure for chymotrypsin activity measurements by AuNPs-peptide probe

For the standard chymotrypsin activity assay, chymotrypsin (25 kDa) prepared in 1 mM HCl with 2 mM $CaCl_2$ and stored at −20 °C. Different concentrations of chymotrypsin were diluted with pH 8.0 TTC buffer and added into AuNPs-peptide probe (125 μL) to comprise 250 μL of mixture, and then incubated at 37 °C. All of the solutions were analyzed with fluorescence spectrophotometer (Hitachi F-2700), using excitation/emission at 495/515 nm. Delta fluorescence intensity is the difference of recovered fluorescence between protease-activated AuNPs-peptide probe and non-activated control group.

4-8. Animals

Female C57BL/6 mice, purchased from the National Laboratory Animal Center (NLAC, Taipei, Taiwan), were housed at the Laboratory Animal Center, National Chiao Tung University, under standard conditions. Female mice of 6 to 8 weeks of age were used in this study. All experimental procedures were carried out in accordance with the guidelines of the Institutional Animal Care and Use Committee of National Chiao Tung University. Every effort was made to minimize the suffering of the animals and the number of animals used.

4-9. Cerulein-induced AP mouse model

The cerulein-induced AP mouse model was developed according to a previous protocol,[43] with minor modifications. The mice were induced to develop AP by 4 doses of intraperitoneal injections of cerulein (200 μg kg^{-1}) at 2 h intervals. Each group consisted of four mice. The control subjects were equally treated with 0.9% NaCl (10 μL mg^{-1} 2 h^{-1}, 4 IP injections). The mice were sacrificed at 8, 10, or 24 h after the first administration of saline (as a control) or cerulein. Mice were fasted for 6 h prior to sacrifice, after which the blood, duodenum, and pancreas were collected.

For the time courses of fecal chymotrypsin in AP model experiments, the mice were divided into two groups. All mice were subjected to 12 h fasting prior to injections. AP ($n = 4$) was induced by 4 doses of cerulein (200 μg kg^{-1} 2 h^{-1}), and the control subjects ($n = 3$) were equally treated with 0.9% NaCl (10 μL mg^{-1} 2 h^{-1}). All feces were subjected to lysis as previously described.

4-10. Sample collection

For the fecal chymotrypsin assay, the feces were weighed and preserved at 4 °C before extraction. The fecal protein extraction process was as follows: one feces (10–25 mg per feces) was dissolved in 0.5 mL fecal protein extraction buffer (250 mM NaCl, 50 mM $CaCl_2$, and 0.25% Triton X-100) for 5 min with continuously mixing by vortex mixer followed by centrifugation (10 000 × g, 1 min), and then the supernatant was collected.

For the chymotrypsin assays in the duodenal eluent and pancreas, the mice were sacrificed with CO_2 inhalation. Blood was collected by direct cardiac puncture and mixed with heparin to acquire plasma after centrifugation (3000 × g, 10 min at 4 °C). The first part of the small intestine followed the demarcation set by Shang[44] to determine the duodenum. The duodenal contents were eluted with 1 mL DPBS and collected the eluent. The duodenal eluent was treated by centrifugation (13 000 × g, 10 min at 4 °C), and the supernatants were collected. The pancreas tissues were homogenized with 1 mL PRO-PREP protein extraction solution (iNtRON Biotechnology, Seongnam, South Korea). The homogenates were centrifuged at 13 000 × g for 10 min at 4 °C. All the supernatants were collected and stored at −80 °C until further analysis. The protein concentrations of the supernatant were measured using a Bio-Rad protein assay (Bio-Rad Laboratories, Hercules, CA, USA).

4-11. Statistical analysis

All data were reported as the mean ± standard deviation (SD) for the specified number of replicates indicated in the caption. Statistical significance was determined by a two-tailed Student's t-test with 95% confidence for unpaired observations. A p value less than 0.05 was considered to be significant.

5. Conclusions

Chymotrypsin can be used as an indicator of pancreatic function. The established AuNPs-peptide probe was used in chymotrypsin assays showing high sensitivity at the pg mL^{-1} level and requiring only 15 min to detect enzyme activity. The sensitivity of the AuNPs-peptide probe was greatly increased through the use of a spacer-enhanced polyvalent peptide, $(Asp)_5$. This process is a one-step biological recognition element assembly procedure that circumvents the use of additional stabilizers and enhances stability.

A cerulein-induced AP mouse model was established in this study, and the AuNPs-peptide probe was successfully used to analyze chymotrypsin activity to assess pancreatic function. The plasma amylase and lipase levels were compared to the chymotrypsin activities in the duodenal eluent, the pancreas and the feces. The increase in pancreatic chymotrypsin activity indicated the pre-activation of trypsin in AP. Meanwhile, the chymotrypsin activity in the duodenal eluent provided a direct

index for the estimation of pancreatic injury, although it required an invasive procedure. The fecal chymotrypsin assay serves as a non-invasive method for the diagnosis of AP, and the fecal chymotrypsin below 30 ng mg^{-1} of stool suggests AP. The AuNPs-peptide probe was successfully applied in the rapid detection of pancreatic disease-related chymotrypsin activity. Moreover, the AuNPs-peptide probe could potentially be used to monitor the leakage of pancreatic juice during surgery to avoid postoperative pancreatic fistulas. This study also provides a platform that could be applied in the daily monitoring of fecal chymotrypsin activity and is non-invasive. This is the first study to use AuNPs-peptide probes in practical disease diagnosis.

Acknowledgements

This work was supported by grants NSC 98-2313-B-009-002-MY3 and NSC 101-2313-B-009-001-MY3 from the National Science Council of Taiwan. This paper (work) was particularly supported by the "Aiming for the Top University Program" of the National Chiao Tung University and Ministry of Education, Taiwan, R.O.C. (MMH-CT-10308).

References

1 L. Goldman, A. I. Schafer and R. L. F. Cecil, *Goldman's Cecil Medicine*, Elsevier/Saunders, Philadelphia, 24 edn, 2012, pp. 937–944.
2 W. Halangk and M. M. Lerch, *Clin. Lab. Med.*, 2005, **25**, 1–15.
3 C. Dervenis, C. D. Johnson, C. Bassi, E. Bradley, C. W. Imrie, M. J. McMahon and I. Modlin, *Int. J. Pancreatol.*, 1999, **25**, 195–210.
4 J. M. Steiner, The Veterinary clinics of North America, *J. Small Anim. Pract.*, 2003, **33**, 1181–1195.
5 P. A. Sutton, D. J. Humes, G. Purcell, J. K. Smith, F. Whiting, T. Wright, L. Morgan and D. N. Lobo, *Ann. R. Coll. Surg. Engl.*, 2009, **91**, 381.
6 R. W. Fallat, J. W. Vester and C. J. Glueck, *JAMA, J. Am. Med. Assoc.*, 1973, **225**, 1331–1334.
7 E. E. Argueta and K. M. Nugent, *ICU Director 4.4*, 2013, 166–169.
8 K. Ko, L. C. Tello and J. Salt, *The Medicine Forum*, 2011, **11**(1), 4.
9 R. M. Ayling, *Ann. Clin. Biochem.*, 2012, **49**(1), 44–54.
10 N. F. Adham, B. J. Dyce, M. C. Geokas and B. J. Haverback, *Am. J. Dig. Dis.*, 1967, **12**, 1272–1276.
11 D. M. Goldberg, *Clin. Chim. Acta*, 2000, **291**, 201–221.
12 I. Molinari, K. Souare, T. Lamireau, M. Fayon, C. Lemieux, A. Cassaigne and D. Montaudon, *Clin. Biochem.*, 2004, **37**, 758–763.
13 J. G. Lieb Ii and P. V. Draganov, *World J. Gastroenterol.*, 2008, **14**, 3149.
14 C. J. Mu, D. A. LaVan, R. S. Langer and B. R. Zetter, *ACS Nano*, 2010, **4**, 1511–1520.
15 S. B. Lowe, J. A. G. Dick, B. E. Cohen and M. M. Stevens, *ACS Nano*, 2012, **6**, 851–857.
16 Y. P. Kim, Y. H. Oh, E. Oh, S. Ko, M. K. Han and H. S. Kim, *Anal. Chem.*, 2008, **80**, 4634–4641.
17 M. Swierczewska, S. Lee and X. Chen, *Phys. Chem. Chem. Phys.*, 2011, **13**, 9929–9941.
18 K. Kang, J. Wang, J. Jasinski and S. Achilefu, *J. Nanobiotechnol.*, 2011, **9**, 1–13.
19 C. S. Yun, A. Javier, T. Jennings, M. Fisher, S. Hira, S. Peterson, B. Hopkins, N. O. Reich and G. F. Strouse, *J. Am. Chem. Soc.*, 2005, **127**, 3115–3119.
20 T. L. Jennings, M. P. Singh and G. F. Strouse, *J. Am. Chem. Soc.*, 2006, **128**, 5462–5467.
21 M. Fanun, *Colloids in biotechnology*, Taylor & Francis Group, 2010.
22 R. Lévy, N. T. K. Thanh, R. C. Doty, I. Hussain, R. J. Nichols, D. J. Schiffrin, M. Brust and D. G. Fernig, *J. Am. Chem. Soc.*, 2004, **126**, 10076–10084.
23 J. A. Tullman, W. F. Finney, Y. J. Lin and S. W. Bishnoi, *Plasmonics*, 2007, **2**, 119–127.
24 K. M. Harkness, B. N. Turner, A. C. Agrawal, Y. Zhang, J. A. McLean and D. E. Cliffel, *Nanoscale*, 2012, **4**, 3843–3851.
25 I. Olmedo, E. Araya, F. Sanz, E. Medina, J. Arbiol, P. Toledo, A. AÁlvarez-Lueje, E. Giralt and M. J. Kogan, *Bioconjugate Chem.*, 2008, **19**, 1154–1163.
26 S. Guerrero, J. R. Herance, S. Rojas, J. F. Mena, J. D. Gispert, G. A. Acosta, F. Albericio and M. J. Kogan, *Bioconjugate Chem.*, 2012, **23**, 399–408.
27 R. Greenwood and K. Kendall, *J. Eur. Ceram. Soc.*, 1999, **19**, 479–488.
28 K. Park, J. Jeong and B. H. Chung, *Chem. Commun.*, 2012, **48**, 10547–10549.
29 E. Hutter and D. Maysinger, *Trends Pharmacol. Sci.*, 2013, **34**, 497–507.
30 X. Wang, O. Ramström and M. Yan, *Anal. Chem.*, 2010, **82**, 9082–9089.
31 L. Liu, K. Xu, H. Wang, P. K. J. Tan, W. Fan, S. S. Venkatraman, L. Li and Y.-Y. Yang, *Nat. Nanotechnol.*, 2009, **4**, 457–463.
32 C. Tassa, J. L. Duffner, T. A. Lewis, R. Weissleder, S. L. Schreiber, A. N. Koehler and S. Y. Shaw, *Bioconjugate Chem.*, 2009, **21**, 14–19.
33 W. R. Algar, A. Malonoski, J. R. Deschamps, J. B. Blanco-Canosa, K. Susumu, M. H. Stewart, B. J. Johnson, P. E. Dawson and I. L. Medintz, *Nano Lett.*, 2012, **12**, 3793–3802.
34 N. O. Fischer, C. M. McIntosh, J. M. Simard and V. M. Rotello, *Proc. Natl. Acad. Sci. U. S. A*, 2002, **99**, 5018–5023.
35 Y. C. Chuang, W. T. Huang, P. H. Chiang, M. C. Tang and C. S. Lin, *Biosens. Bioelectron.*, 2012, **32**, 24–31.
36 Z. Piotrowski, P. Myśliwiec, M. Gryko, H. Ostrowska and M. Baltaziak, *Rocz. Akad. Med. Bialymstoku*, 2003, **48**, 61–65.
37 A. A. Aghdassi, J. Mayerle, S. Christochowitz, F. U. Weiss, M. Sendler and M. M. Lerch, *Fibrog. Tissue Repair*, 2011, **4**(1), 26.
38 S. Yamashita, M. Sakabe, T. Ishizawa, K. Hasegawa, Y. Urano and N. Kokudo, *Br. J. Surg.*, 2013, **100**, 1220–1228.
39 J. G. Banwell, P. J. Leonard and R. M. F. Lobo, *Gut*, 1965, **6**, 143–145.
40 J. G. Lieb and P. V. Draganov, *World J. Gastroenterol.*, 2008, **14**, 3149–3158.

41 Y. C. Chuang, J. C. Li, S. H. Chen, T. Y. Liu, C. H. Kuo, W. T. Huang and C. S. Lin, *Biomaterials*, 2010, **31**, 6087–6095.
42 D. H. Tsai, M. P. Shelton, F. W. DelRio, S. Elzey, S. Guha, M. R. Zachariah and V. A. Hackley, *Anal. Bioanal. Chem.*, 2012, **404**, 3015–3023.
43 M. Tsai, C. Chen, S.-H. Chen, Y. Huang and T. Chiu, *J. Gastroenterol.*, 2011, **46**, 822–833.
44 L. Shang, N. Thirunarayanan, A. Viejo-Borbolla, A. P. Martin, M. Bogunovic, F. Marchesi, J. C. Unkeless, Y. Ho, G. C. Furtado, A. Alcami, M. Merad, L. Mayer and S. A. Lira, *Gastroenterology*, 2009, **137**, 1006–1018.